Nanodiamonds do not provide unique evidence for a Younger Dryas impact

H. Tian[a], D. Schryvers[a,1], and Ph. Claeys[b]

[a]Electron Microscopy for Materials Science (EMAT), Department of Physics, University of Antwerp, Groenenborgerlaan 171, B-2020 Antwerp, Belgium; and [b]Earth System Science, Vrije Universiteit Brussel, Pleinlaan 2, B-1050 Brussels, Belgium

Edited by Mark H. Thiemens, University of California, San Diego, CA, and approved November 19, 2010 (received for review June 20, 2010)

Microstructural, $\delta^{13}C$ isotope and C/N ratio investigations were conducted on excavated material from the black Younger Dryas boundary in Lommel, Belgium, aiming for a characterisation of the carbon content and structures. Cubic diamond nanoparticles are found in large numbers. The larger ones with diameters around or above 10 nm often exhibit single or multiple twins. The smaller ones around 5 nm in diameter are mostly defect-free. Also larger flake-like particles, around 100 nm in lateral dimension, with a cubic diamond structure are observed as well as large carbon onion structures. The combination of these characteristics does not yield unique evidence for an exogenic impact related to the investigated layer.

transmission electron microscopy | diffraction | spectroscopy

Recently, the presence of different types of diamond morphologies and structures in a black carbon-rich sedimentary layer has been used as evidence to support an extraterrestrial impact approximately 12.9 ka ago as the cause of the Younger Dryas climate change (1–3). These authors argue that shock metamorphism produced these diamond particles (2). Other arguments from the same authors supporting the suggestion of an extraterrestrial impact at the Younger Dryas are, amongst others, high concentrations of Ir, magnetic microspherules and grains and carbon spherules. However, strong doubts still exist about the nature and implications of these markers. Indeed, Paquay et al. (4) in 2009 failed to reproduce the elevated concentrations of platinum group elements (including Ir) reported by Firestone et al. (3). Moreover, the same authors showed that $^{187}Os/^{185}Os$ isotopic ratios, considered to being the most sensitive indicator of a meteoritic contribution, yield values typical of the terrestrial crust. Surovell et al. (5) also failed to confirm enhanced levels of impact microspherules in the Younger Dryas unit from seven different sites. Also, the recent electron microscopy data presented to prove the existence of Lonsdaleite particles with crystallographic defects, claimed to be due to impact-related shock transformation, is not convincing (2). Although the reported lattice parameters can indeed be assumed to originate from Lonsdaleite, low precision measurements from ring patterns resulting from small particles can at most be seen as a first indication. This uncertainty was recently confirmed by an extensive study by Daulton et al. (6) who compared the Kennett et al. electron diffraction data (2) with different graphene morphologies and simulated Lonsdaleite diffraction. The lack of any experimental intensity at expected Lonsdaleite lines such as 102 indicates that no such structure appears in the investigated samples. In fact, the occurrence of asymmetric double diffraction lines points to the existence of graphene/graphane aggregates, also explaining all other observed rings. Also, no two-beam or high-resolution lattice images were presented by Kennet et al. to support their interpretation of stacking faults in the Lonsdaleite crystals.

In the present work, we focus on diamond particles and carbon isotope values in material obtained from excavations in Lommel (Belgium), in which the Younger Dryas unit or boundary (YDB) is revealed as a thin black layer as shown in Fig. 1. The same layer was also included in the original paper claiming the extraterrestrial impact (3) and in the recent confronting study of Paquay et al. (4). The thickness and depth of this black layer vary depending on the actual location investigated along the excavated trench. At most places, the layer is buried under approximately 50 cm of yellow clay whereas 1 m thick, fine white sands occur underneath. Samples of this black layer essentially composed of carbon, as well as samples from parts of the immediately over- and underlying sediments, were investigated by different modes of transmission electron microscopy (TEM) and $\delta^{13}C$ isotope measurements to document the crystallography and possibly the formation process of the diamond particles as well as the origin of the C matter present in this layer.

Fig. 1. Depth location of the black Younger Dryas Boundary at Lommel, Belgium.

Results

Our findings confirm, and in fact reveal more direct proof than the earlier studies, the existence of diamond nanoparticles also in this European YDB layer. No such particles are found in the overlying silt and clay or in the underlying fine sands. The latter contain, aside from the prevalent amorphous carbon material, the expected silicates and calcites with some of those also occasionally observed in samples of the black layer. In contrast to the reports from other YDB sites (3) the Lommel black layer samples did not contain any millimeter-sized foam-like carbon spherules. Because such spherules are relatively brittle due to a high degree of porosity of the carbon skeleton, a possible reason for the lack of such large particles in the Lommel layer could be the action of diagenesis through which the particles are crushed under the weight of the upper soil layers. On the other hand, any existing diamond material in such spherules, as found before in carbon spherules collected in undisturbed upper soils (7) from Belgium and Germany, would still be present in the Lommel black layer.

Author contributions: D.S. and Ph.C. designed research; H.T. performed research; H.T., D.S., and Ph.C. analyzed data; and D.S. and Ph.C. wrote the paper.

The authors declare no conflict of interest.

This article is a PNAS Direct Submission.

[1]To whom correspondence should be addressed. E-mail: nick.schryvers@ua.ac.be.

www.pnas.org/cgi/doi/10.1073/pnas.1007695108

Most of the material observed in the Lommel TEM samples consists of amorphous carbon, as expected from the black nature of the layer. However, several crystalline particles can be identified within this amorphous material. In Fig. 2*A* a relatively large crystalline particle with lateral sizes of around 100 nm is shown, together with the corresponding selected area electron diffraction (SAED) pattern (Fig. 2*B*). When measuring the g-vectors of the diffraction spots, the indexing corresponds with the [001] zone of cubic diamond with the typical diamond extinctions at the ⟨200⟩ positions. The latter are often not recognized in ring patterns of groups of small particles due to incomplete extinction conditions (1, 2). In fact, this is undisputable proof of diamond in its classic cubic form found in YDB material and which, to our knowledge, was never reported before.

The second proof of the cubic diamond character of this large particle is the electron energy loss near edge spectrum (ELNES) shown in Fig. 2*C*. The carbon K-edge with an onset around 285 eV first shows a small π^* edge from supporting or covering amorphous carbon but the three typical small maxima of the σ^* edge between 300 and 315 eV followed by a shallow bump at around 330 eV are a clear fingerprint for cubic diamond (7–9). Indeed, recent density functional theory calculations have shown that the ELNES patterns from other carbon allotropes such as Lonsdaleite and face-centered cubic (FCC) carbon clearly differ from the one presented below (9). For example, the peak at around 20 eV above the onset, clearly visible in Fig. 2*C*, does not appear for the hexagonal Lonsdaleite structure.

In Fig. 2*D* a Fourier filtered atomic resolution image of the same particle along the same [001] zone reveals the cubic symmetry of the atomic lattice with the typical 0.126 nm for the 220 interplanar spacing. The fact that the latter image resolution can be obtained in conventional high-resolution work implies that the present object cannot be much thicker than 20 or 30 nm. As such, this large diamond particle can be considered as a diamond flake similar to those found in the carbon spherules obtained from undisturbed top-soils in Belgium and Germany investigated in an earlier study (see, e.g., figure 8 in ref. 7). No twins or stacking faults are seen in this particle but in the present selected region, an edge dislocation with Burgers vector 1/2[110] is visible in the crystal lattice, again similar to the flake observed in the spherules (7).

Smaller nanoparticles, with a typical diameter of ~20 nm, have also been observed. The averaged ELNES pattern is shown in Fig. 3*A*, again revealing the typical cubic diamond fingerprint. The diamond peaks are now less sharp than in the case of the diamond flake of Fig. 2, which can be understood from the abundance of the amorphous background material, also revealed in the spectrum by a higher π^* edge. The nanoparticles are shown in Fig. 3 *B–D* using selected energy filtered transmission electron microscopy (EFTEM) mapping: In Fig. 3*B* the so-called zero-loss image is shown, revealing the actual location of strongly scattering material such as crystalline nanoparticles. Fig. 3*C* is an image formed with the electrons in the π^* edge whereas the σ^* edge was selected to form the image in Fig. 3*D*. Observing dark regions at the same locations as the particles when using the π^* peak implies that these areas contain relatively less amorphous π^* material. On the other hand, the brighter regions in Fig. 3*D* confirm the cubic diamond type of the particles with a corresponding σ^* shape.

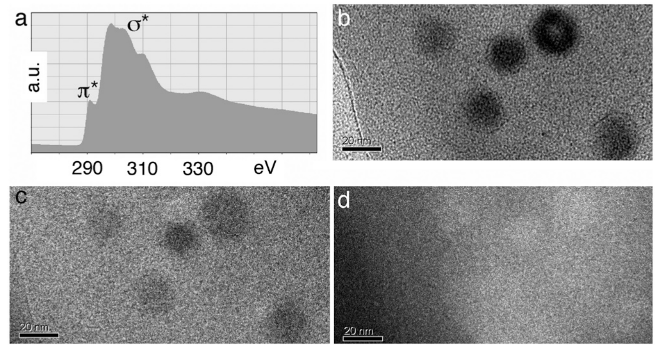

Fig. 3. (*A*) ELNES of a region with many nanoparticles. EFTEM maps using electrons from the (*B*) zero-loss, (*C*) π^* and (*D*) σ^* regions.

The close-to-spherical and relatively large cubic diamond particle shown in Fig. 4*A* exhibits five-fold twinning close to one of its edges. Observation of such star-like twinning in FCC-based structures is often interpreted as an indication of isotropic growth (10, 11). In the present case the asymmetric location of the star center could, however, indicate some preferential growth conditions. In Fig. 4*B* another large particle with a single twin is shown. Smaller nanoparticles, below 5 nm, did not reveal any twinning. Also, no dislocations were observed in any of these nanoparticles.

A completely different carbon structure, a so-called carbon onion or onion ring, is shown in Fig. 5*A*, with part of the image being magnified in Fig. 5*B* for clarity. The average interplanar spacing between two successive rings measured from such high resolution transmission electron microscopy (HRTEM) images from different onion rings in the Lommel YDB material varies between 0.268 and 0.284 nm. These values are substantially smaller than the regular graphite interlayer distance of 0.341 nm (12). Such reduced interlayer distances can yield internal pressures up to 100 GPa in the inside of the carbon onion. The onion in Fig. 5 is a very large example, with over 50 graphene sheets and a diameter above 25 nm (a double arrow reveals one radial direction toward the only visible edge part, edges on the left and below extend beyond the field of view). The graphene sheets also continue very far toward the center, indicated by the single arrow on Fig. 5*A*, although the actual structure (amorphous or crystalline) of the core cannot be resolved. The close-to-circular symmetry and the sharp interlayer distance are evidenced by the fast Fourier transform (FFT) inset. A stacking defect can be observed in the highlighted rectangle of a magnified part in Fig. 5*B*. In view of the present interest in nanodiamond, it is important to note that

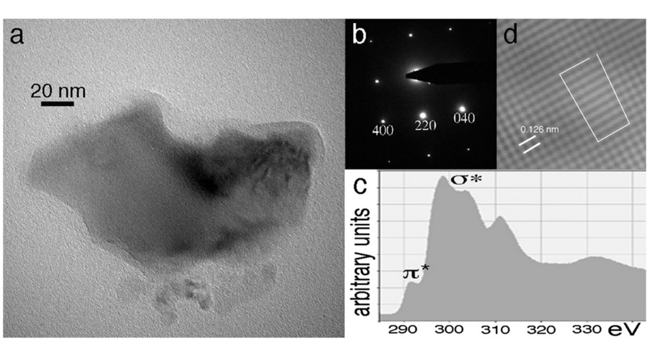

Fig. 2. (*A*) Flake-like diamond particle with (*B*) [001] SAED pattern revealing cubic diamond extinctions at ⟨200⟩, (*C*) HRTEM image revealing an edge dislocation and (*D*) ELNES with typical diamond fingerprint.

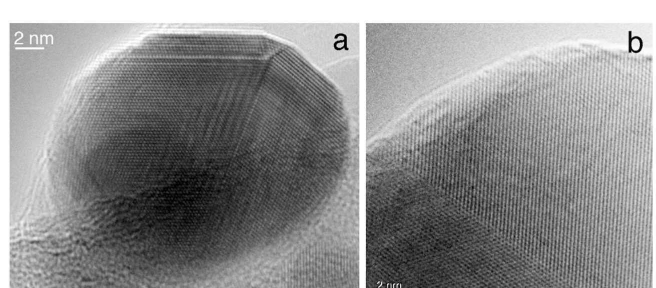

Fig. 4. (*A*) Close-to-spherical nanoparticle with five-fold twinning and (*B*) single twin in large particle.

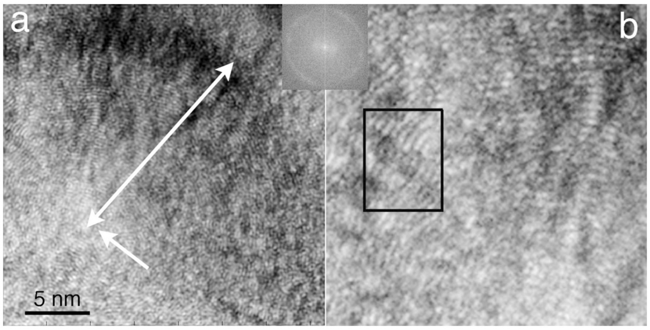

Fig. 5. (*A*) Carbon onion with compressed interplanar spacings between 0.268 nm and 0.284 nm [with magnified part and highlight of defect region for clarity in (*B*)]. The single arrow indicates the center of the onion and the double arrow its radius. The inset is an FFT revealing the close-to-circular symmetry and sharp interlayer distance.

such carbon onions can act as nanoscopic pressure cells for the formation of diamond nanoparticles in the core of the onion structure (13, 14). Due to the size of the onions yielding severe overlapping of above and below curved sheets plus the surrounding amorphous carbon, the images are unfortunately not sufficiently clear for any further structural conclusion, even after applying image processing.

In view of earlier reports of Lonsdaleite with respect to impact-related material, we deliberately looked for hexagonal diffraction patterns with the proper lattice parameters in our samples. However, no indications of such a structure were found, not in the present material from Lommel [nor in some revisited samples from the spherules collected from undisturbed upper soils (7)]. In these experiments special care was taken to avoid any effects of the high voltage electron beam in the TEM, which might damage or even transform the Lonsdaleite back into graphite due to the instability of this structure.

Also carbon isotope measurements and C/N values were determined from the black material of the Lommel YDB layer. The nanodiamond particles in the present material could not be analyzed separately because of their small size. The Lommel samples were thus analyzed in aliquots of increasingly smaller and smaller size fractions (down to ∼10 μg C) in an attempt to eventually detect an effect driven by the presence of extraterrestrial organic material. The δ^{13}C and C/N values remain constant through the experiment and generated δ^{13}C values between −28.1 and −26.3‰, and C/N ratios between 9.2 and 26.9.

Discussion

Comparing the findings of the present work with those in the top-soil spherules (7), those from Kennett et al. (1, 2) and other meteorite findings (15–18), leads to the following remarks. Both micron-sized flakes and nanoparticles of cubic diamond are present in the Lommel YDB material and the top-soil spherules. However, there is no report of flakes or excessively thin cubic diamond in meteoritic or impact diamonds. The smallest nanoparticles, up to a few nm in diameter, do not contain any one- or two-dimensional crystal defects in either the Lommel or top-soil cases. Larger sized nanoparticles, around 20 nm diameter, revealing multiple twinning were only observed in the Lommel samples, whereas in the top-soil spherules the larger agglomerates consist of nanostructured grains with strongly deformed crystal lattices (7). Moreover, most twins in the Lommel particles appear in a nonlinear fashion, even star-like, indicating a close-to isotropic type of growth. The larger flakes, around 100 nm in lateral dimension, do not reveal any twins. Stacking faults were not observed in either of our samples. Kennett et al. (1, 2) reported no twinned particles or flakes. The details of the observations on the diamond in the carbon spherules from undisturbed top-soils were attributed to a CVD type growth process, rather than to explosion related phenomena (7).

A very comprehensive work on twinned diamond nanoparticles from meteoritic material was performed by Daulton et al. (15) who compared artificial shock-synthesized (by detonation) and low-pressure chemical vapour deposition (CVD) material with residues from the primitive Allende and Murchison carbonaceous meteorites. One important conclusion was the similarity between the CVD and meteoritic material in view of the number and type of twinned particles. In the present study, most larger particles [i.e., with diameters above 10 nm (but excluding the flakes)], show some kind of twinning (mostly five-fold star, some parallel), the smaller ones being defect-free. Especially the dominant nonlinear character of the observed twins, points to an isotropic growth mechanism for the nanoparticles, possibly of the CVD type in contrast to the detonation type.

In the same work, Daulton et al. (15) also looked at dislocations, but did not find any in the meteoritic or CVD samples. The shock-synthesized material, however, did reveal clear signs of dislocation defects, be it in nano-particles instead of in flakes of the size observed in the Lommel samples. Such dislocations were interpreted as resulting from a martensitic-like transformation from graphite to diamond (19). This could imply a shock-related history for the flakes, where their microscopic shapes could be seen as a remnant of a shock wave front passing through the material. Although the latter is indeed a possible and likely interpretation in the case of particles of known origin, other potential pathways to produce dislocations in the flakes could easily be envisaged, including lattice misfits during epitaxial deposition and growth and strain hardening during deformation. Moreover, more recent work on nanodiamond from detonation experiments also did not reveal any flake-like shapes (20), whereas the type of twinning confirmed the observations by Daulton et al. (15).

Double-check of both the present material and the top-soil spherules for crystallites with a hexagonal symmetry did not reveal Lonsdaleite in either of those. According to Daulton et al. (15), Lonsdaleite nanocrystals are relatively stable in the electron beam, so little or no back-transformation to graphite during observation is expected. The YDB material reported on by Kennett et al. revealed cubic diamond nano- as well as microparticles. In the most recent report by Kennett et al. the existence of Lonsdaleite was identified on the basis of electron diffraction patterns (2). The images of these particles seem to correspond to the flake morphology. However, recent work by Daulton et al. (6) clearly shows that the diffraction rings observed by Kennet et al. (2) can also be explained by graphene/graphane aggregates whereas a 102 ring expected for Lonsdaleite was not observed. Kennet et al. also claimed the observation of stacking faults, but the experimental evidence cannot be considered as very convincing. From the lack of Lonsdaleite in our present material and the results from Daulton et al. (6, 15) it is concluded that no shock-induced metamorphism has occurred when the Lommel material was formed. Alternatively, the flake shape could be a remnant of a deposition and delamination process during which some dislocations are formed by the respective mechanisms proposed above.

The carbon onions observed in the Lommel material are relatively large and can consist of around 50 graphene sheets yielding a diameter of around 25 nm and containing several stacking defects in their shell structure. In most other cases where carbon onions have been observed, they usually have a much smaller diameter and consist of only a few graphene sheets depending on the processing history. An example hereof are the carbon onion structures with diameters below 10 nm observed in artificially produced wood charcoal (21). The latter were attributed to the carbonization of lignin structures in the raw wood starting material. Larger rounded graphitic structures have recently been observed in modern and fossilized charcoal structures indicating a large preservation time after a formation during natural wild

Table 1. Data ranges for $\delta^{13}C$ (‰), C/N ratio and Ir (pg/g) for terrestrial material, extraterrestrial material and the black layer in Lommel (reference numbers are given in brackets) (OM = organic matter**)**

	$\delta^{13}C$ (‰)	C/N	Ir (pg/g)
Terrestrial	−40 to 5 (29, 30) OM & diamond	5 to 70 (31) OM	10 to 80 (4) cont. crust
Extraterrestrial	−38.8 to −32.5 (32) chondrite nanodiamond	75 to 555 (32) chondrite nanodiamond	10^3 to 10^5 (4) impact layers
Lommel black layer	−28.1 to −26.3	9.2 to 26.9	20 to 42 (4)

fires (22). These consist of a shell of about 20 curved graphene sheets surrounding a large amorphous carbon core with diameters up to 50 nm or more, distinguishing them to some extend from the present onion rings in which graphene sheets can still be recognized very close to the center of the onion structure. Such large onion structures can be formed through self-assembly of carbon atoms under electron irradiation of graphitic materials, such as polyhedral carbon particles (13, 14), by thermobaric fullerene processing at 15 GPa and 1100 K (23, 24) or by applying an arc-discharge between two carbon electrodes under water (25, 26).

However, the structural characteristics of the observed carbon onions are insufficient to further conclude on a possible formation history. A mechanism including bombardment of graphitic materials with charged particles could be envisaged in the vicinity of stars, implying an exogenic formation. In fact, these types of carbon structures have indeed been proposed as carriers of the 217.5 nm interstellar UV absorption feature (27). On the other hand, fullerenes have recently also been recorded to exist in interstellar space (28) whereas the pressure and temperature conditions needed to transform those into carbon onions could occur during impact. However, discharges in volcanic or other ash clouds may yield similar features as those produced by the controlled experiments using carbon electrodes. In other words, the occurrence of large carbon onions in the Lommel YDB material is insufficient to determine the origin of the carbon material. Still, the observation of carbon onions opens an extra path for the formation of nanodiamonds as it was indeed shown that electron bombardment can produce nanodiamonds in the interior of the carbon onions (13, 14). Whether such a mechanism can be expected to occur in nature is, however, still unclear.

The argument has been put forward that the Younger Dryas event was caused by mega-airbursts in the atmosphere (1–3). This type of megaexplosion at high altitude would explain the absence of a large 12.9-ka-old impact crater in North America. In the case of airbursts, the produced shocked carbon particles most likely consist of extraterrestrial carbon derived from the projectile and incorporated within the Younger Dryas black layer. The $\delta^{13}C$ and C/N values as well as the earlier determined Ir concentrations (4) obtained from the Lommel black material fall completely within the range of terrestrial organic matter (29–31). However, extraterrestrial organic carbon displays a broad range of isotopic compositions that also include those of terrestrial organic matter (32–35). For example, bulk samples of nanodiamonds separates extracted from primitive chondrites yield $\delta^{13}C$ values around −38.8 to −32.5‰ (i.e., close to the range obtained here), but somewhat higher C/N ratios from 75 to 555 (32). Consequently, the results obtained on the Lommel material do not distinguish between terrestrial and extraterrestrial origins for the carbon. However, the argument could be put forward that the C/N ratios appear rather low compared to those of bulk nanodiamonds measured in chondrites (32). Although the $\delta^{13}C$ and C/N ratio cannot be considered as diagnostic, a fully terrestrial origin of the C present in the Lommel black layer is compatible with the clearly crustal signatures of the concentration in platinum group elements (4) and $^{187}Os/^{185}Os$ isotopic ratios determined earlier (36, 37). Part of this is listed in Table 1 and schematically shown in Fig. 6 where numerical values for the $\delta^{13}C$, C/N and Ir parameters are compared with representative data from known meteoritic and terrestrial material, revealing that the entire Lommel data range fits inside the terrestrial range and does not overlap with the extraterrestrial data. This data thus implies that the present materials and formation mechanisms should primarily be correlated with particular activities on earth, rather than with exogenic origins.

We conclude that the Younger Dryas boundary carbon material excavated in Lommel, Belgium, contains cubic diamond material in different forms. Aside from amorphous carbon, diamond nanoparticles with diameters of a few nm up to a maximum of around 20 nm are the most abundant structures. The smallest ones, below 5 nm diameter, are defect-free whereas the larger ones often contain twins with nonlinear configurations being dominant. The latter points toward an isotropic growth mechanism, possibly CVD type. Also flake-like cubic diamond particles of up to 100 nm in lateral dimensions have been found. This particular shape as well as the occasional observation of dislocations

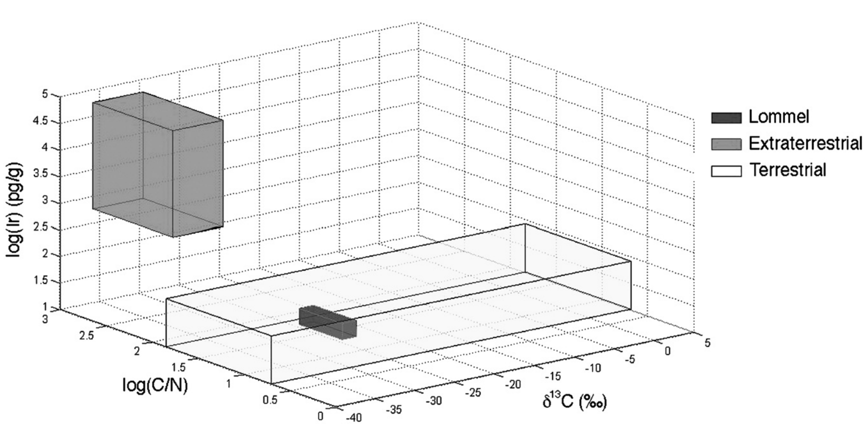

Fig. 6. Schematic representation of the ranges of $\delta^{13}C$, C/N ratio and Ir concentration for terrestrial crust (white), chondritic meteorites (gray), and Lommel black layer material (black). The overlap between terrestrial crust and Lommel material is apparent whereas the extraterrestrial material is clearly separated from the other two.

could indicate a martensitic-like transformation path from graphite to diamond, although epitaxial growth cannot be ruled out. Because no hexagonal diamond (Lonsdaleite) could be identified a shock-induced mechanism is unlikely to be involved in the formation of the crystalline carbon material in the present layer. The observed large carbon onion structures could be produced by a variety of processes, which implies that their exact origin remains unclear. Graphitic ring structures can indeed be formed during natural processes such as wild fires, although the existing observations reveal slightly different morphologies. As a final conclusion it should be stated that the present variety of crystalline structures observed in the black Younger Dryas boundary in Lommel does not provide sufficient evidence to conclude an exogenic impact as the origin of these structures.

Materials and Methods

The material was collected on-site by one of the authors (D.S.) and small parts of the excavated material was crushed in ethanol and dispersed on holey carbon TEM grids. High-resolution TEM imaging as well as electron energy loss spectroscopy were performed with an FEI CM30 ultratwin field emission gun instrument operating at 300 keV equipped with a postcolumn GIF200 spectrometer. Background subtraction and zero-loss convolution of the spectra were obtained via the GATAN DM software.

Carbon and nitrogen content along with carbon isotope signature ($\delta^{13}C$) were determined by combusting preweighed crushed samples, acidified to remove $CaCO_3$, and contained in silver cups in a Flash1112 elemental analyzer coupled to a Delta + XL via a conflo III interface (Thermo Scientific). Internal reference materials included IAEA-CH6 for C whereas acetanilide was used for total organic carbon and total nitrogen calibration. Typical reproducibility of $\delta^{13}C$ is ± 0.2‰.

1. Kennett DJ, et al. (2009) Nanodiamonds in the Younger Dryas boundary sediment layer. *Science* 323:94–94.
2. Kennett DJ, Kennett JP, West A, West GJ, Bunch TE (2009) Shock-synthesized hexagonal diamonds in Younger Dryas boundary sediments. *Proc Natl Acad Sci USA* 106:12623–12628.
3. Firestone RB, West A, Kennett JP, Becker L, Bunch TE (2007) Evidence for an extraterrestrial impact 12,900 years ago that contributed to the megafaunal extinctions and the Younger Dryas cooling. *Proc Natl Acad Sci USA* 104:16016–16021.
4. Paquay FS, Goderis S, Ravizza G, Vanhaeck F, Boyd M (2009) Absence of geochemical evidence for an impact event at the Bølling–Allerød/Younger Dryas transition. *Proc Natl Acad Sci USA* 106:21505–21510.
5. Surovell T, Holliday VT, Gingericha JAM, Ketrona C, Haynes CV (2009) An independent evaluation of the Younger Dryas extraterrestrial impact hypothesis. *Proc Natl Acad Sci USA* 106:18155–18158.
6. Daulton TL, Pinter N, Scott AC (2010) No evidence of nanodiamonds in Younger Dryas sediments to support an impact event. *Proc Natl Acad Sci USA* 107:16043–16047.
7. Yang ZQ, et al. (2008) TEM and Raman characterisation of diamond micro- and nanostructures in carbon spherules from upper soils. *Diamond &; Related Materials* 17:937–943.
8. Egerton RF (1996) *Electron Energy-Loss Spectroscopy in the Electron Microscope* (Plenum, New York).
9. Dadsetani M, Titantah JT, Lamoen D (2010) Ab initio calculation of the energy-loss near-edge structure of some carbon allotropes: Comparison with n-diamond. *Diam Relat Mater* 19:73–77.
10. Matsumoto S, Matsui Y (1983) Electron microscopic observation of diamond particles grown from the vapour phase. *J Mater Science* 18:1785–1793.
11. Kimoto K, Nishida I (1967) Multiply twinned particles of F.C.C. metals produced by condensation in argon at low pressures. *J Phys Soc Jpn* 22:940–940.
12. Brown TE, LeMay HE, Bursten BE (1997) *Chemistry the Central Science*, (Simon & Schuster, Upper Saddle River, NJ), 227, pp 412–413.
13. Banhart F, Pulickel M, Ajayan PM (1997) Self-compression and diamond formation in carbon onions. *Adv Mater* 9:261–263.
14. Banhart F, Ajayan PM (1996) Carbon onions as nanoscopic pressure cells for diamond formation. *Nature* 382:433–435.
15. Daulton TL, Eisenhour DD, Bernatowicz TJ, Lewis RS, Buseck PR (1996) Genesis of presolar diamonds: Comparative high-resolution transmission electron microscopy study of meteoritic and terrestrial nano-diamonds. *Geochim Coscmochim Ac* 60:4853–4872.
16. Goresy El (1968) A new allotropic form of carbon from the Ries crater. *Science* 161:363–364.
17. Blake DF, Freund F, Krishnan KFM, Echer CJ, Shipp R (1988) The nature and origin of interstellar diamond. *Nature* 332:611–613.
18. Lewis RS, Tang M, Wacker JF, Anders E, Steel E (1987) Interstellar diamonds in meteorites. *Nature* 326:160–162.
19. Erskine DJ, Nellis WJ (1991) Shock-induced martensitic phase transformation of oriented graphite to diamond. *Nature* 349:317–319.
20. Turner S, et al. (2009) Determination of size, morphology, and nitrogen impurity location in treated detonation nanodiamond by transmission electron microscopy. *Adv Funct Mater* 19:2116–2124.
21. Hata T, Imamura Y, Kobayashi E, Yamane K, Kikuchi K (2000) Onion-like graphitic particles observed in wood charcoal. *J Wood Sci* 46:89–92.
22. Cohen-Ofri I, Popovitz-Biro R, Weiner S (2007) Structural characterization of modern and fossilized charcoal produced in natural fires as determined by using electron energy loss spectroscopy. *Chem Eur J* 13:2306–2310.
23. Blank VD, Kulnitskiy BA, Perezhogin IA (2009) Structural peculiarities of carbon onions, formed by four different methods: Onions and diamonds, alternative products of graphite high-pressure treatment. *Scripta Mater* 60:407–410.
24. Blank VD, Kulnitskiy BA, Dubitskiy GA, Alexandrou I (2005) The structures of C60-Phases, formed by thermobaric treatment: HREM-studies. *Fuller Nanotub Car N* 13(supp. 1):167–177.
25. Sano N, et al. (2002) Properties of carbon onions produced by an arc discharge in water. *J Appl Phys* 92:2783–2788.
26. Sano N, Wang H, Chhowalla M, Alexandrou I, Amaratunga GAJ (2001) Nanotechnology: Synthesis of carbon "onions" in water. *Nature* 414:506–507.
27. Chhowalla M, et al. (2003) Carbon onions: Carriers of the 217.5 nm interstellar absorption feature. *Phys Rev Lett* 90:155504–1.
28. Cami J, Bernard-Salas J, Peeters E, Malek SE (2010) Detection of C60 and C70 in a young planetary nebula. *Science* 329:1180–1182.
29. Hoefs J (2009) *Stable Isotope Geochemistry* (Springer, New York), 6th ed., p 288.
30. Cartigny P (2005) Stable isotopes and the origin of diamond. *Elements* 1:79–84.
31. Meyers PhA (1994) Preservation of elemental and isotopic source identification of sedimentary organic matter. *Chem Geol* 114:289–302.
32. Russell SS, Arden JW, Pillinger CT (1996) A carbon and nitrogen isotope study of diamond from primitive chondrites. *Meteorit Planet Sci* 31:343–355.
33. Pearson VK, Septhon MA, Franchi IA, Gibson JM, Gilmour I (2006) Carbon and nitrogen in carbonaceous chondrites: Elemental abundances and stable isotopic compositions. *Meteorit Planet Sci* 41:1899–1918.
34. Alexander CMOD, Fogel M, Yabuta H, Gody GD (2007) The origin and evolution of chondrites recorded in the elemental and isotopic compositions of their macromolecular organic matter. *Geochim Coscmochim Ac* 71:4380–4403.
35. McKeegan KD, Aléon J, Bradley J, Brownlee D, Busemann H (2006) Isotopic compositions of cometary matter returned by stardust. *Science* 314:1724–1728.
36. Claeys Ph, Paquay F, Goderis S, Vanhaecke F (2008) Do the concentrations of platinum group elements in the Younger Dryas black layer really support an extraterrestrial origin? *American Geophysical Union, Fall Meeting 2008 Abstract* 89(53):P31A–1382.
37. Koeberl C, Peucker-Ehrenbrink B, Reimold U, Shukolyukov A, Lugmair G (2002) Comparision of the osmium and chromium isotopic methods in the detection of meteoritic components in impactities: Examples from the Morokweng and Vredefort impact structure South Africa. *Geological Society of America, Special Publication* 356:607–617.